K. Volz
e-mail: kerstin.volz@physik.uni-marburg.de

T. Torunski

D. Lackner

O. Rubel

W. Stolz

Material Sciences Center and Department of Physics,
Philipps University,
D-35032 Marburg,
Germany

C. Baur

S. Müller

F. Dimroth

A. W. Bett

Fraunhofer Institute for Solar Energy Systems,
D-79110 Freiburg,
Germany

Material Development for Improved 1 eV (GaIn)(NAs) Solar Cell Structures

The dilute nitride (GaIn)(NAs) *material system grown lattice matched to* GaAs *or Ge with a* 1 eV *band gap is an interesting material for the use in four-junction solar cells with increased efficiencies. As a result of its metastability, several challenges exist for this material system, which up to now limits the device performance. We performed nanostructural analysis in combination with photoluminescence characterization to optimize the metal organic vapor phase growth as well as the annealing conditions for the quaternary solar cell material. The optimum annealing conditions depend strongly on the In content of the quaternary material. Valence force field calculations of stable N environments in the alloy support the model that the N moves from a Ga rich environment realized during growth into an In rich environment upon annealing. Simultaneously, N induced strain fluctuations, which are detected in the N containing material upon growth, are dissolved and the device properties are improved.* [DOI: 10.1115/1.2734568]

Introduction

The novel, metastable compound semiconductor system (GaIn)(NAs) on GaAs introduced by Kondow et al. [1] is gaining increasing interest in recent years due to its unique electronic properties, such as the extreme band-gap bowing and the specific conduction band formation [2,3]. The excellent high-temperature characteristics make this material system very promising for long wavelength (1.3–1.55 μm) laser diodes for optical fiber communications. Aside from these laser applications, potential application of (GaIn)(NAs) in high-efficiency multijunction solar cells is discussed [4]. Significantly higher efficiencies have been theoretically calculated for a 1 eV band gap material, introduced as a third junction in the established two-junction (GaIn)P/GaAs cells. The efficiencies of such a solar cell are predicted to increase from ~26% (AM0) to above 38% (AM0) and even to about 41%, if Ge would be introduced as a fourth junction below this stack. In terrestrial environment, the efficiencies would boost to 47% or 52%, respectively, calculated for AM1.5 and 500 suns [4]. (GaIn)(NAs) would be an optimal candidate as 1 eV solar cell material in multijunction solar cell concepts, as it can be grown lattice matched to GaAs or Ge substrates. Up to now, however, the short minority carrier diffusion in the devices limits the performance of such cells[5–8]. Minority carrier diffusion lengths as low as 10–20 nm have been observed. With minority carrier diffusion lengths shorter than the depletion widths, the carrier collection in such a device is dominated by field-aided collection rather than by diffusion collection, which is common for other III/V materials [9]. This results in low short circuit currents and low quantum efficiencies of the devices. It is crucial to determine whether these short diffusion lengths are due to extrinsic, growth related defects, or are an intrinsic property of this material system. Another important issue in these films is the high *p*-type background carrier concentration on the order of $10^{17}/\mathrm{cm}^3$ [5,6], which is mainly observed for material grown by metalorganic vapor phase epitaxy (MOVPE), influencing the doping characteristics and carrier concentrations, the carrier mobility, as well as the performance of the devices. Main differences between molecular beam epitaxy (MBE) and MOVPE grown material comprise this carbon impurity in MOVPE grown material as well as hydrogen incorporation into MOVPE grown material as a result of the usage of MO sources. Several structural characteristics, as outlined in the following, are intrinsic to the dilute N-containing material systems.

The present paper presents specific intrinsic structural and compositional properties of the metastable quaternary material, such as chain like N ordering in growth direction and an enhanced C incorporation in the material with increasing N content. In addition, this study discusses up to which extent optimized growth and annealing conditions can be found to circumvent these properties of the material and hence improve device performance.

Experiment

All (GaIn)(NAs) bulk structures or multiquantum well samples used for this study have been grown on (100) GaAs substrates in a commercially available horizontal reactor system (AIX200) by MOVPE using hydrogen carrier gas at a low reactor pressure of 50 mbar. Due to the large difference in covalent radius between nitrogen and arsenic, the material system under investigation is metastable, and low substrate temperatures have to be chosen in order to achieve significant N incorporation. Substrate temperatures are usually fixed at 525°C for quantum well samples and to slightly higher temperatures (550°C) in the case where bulk material for solar cell application is grown in order to compensate for

Contributed by the Solar Energy Division of ASME for publication in the JOURNAL OF SOLAR ENERGY ENGINEERING. Manuscript received November 10, 2005; final manuscript received October 23, 2006. Review conducted by Antonio Marti Vega.

the reduced diffusion at the higher growth rate (1 μm/hr) in this case. The substrate temperatures are calibrated to the Al/Si eutectic formation occurring at 577°C. As a consequence of the low growth temperatures, MO sources efficiently decomposing at lower temperatures like the group V sources tertiarybutylarsine (TBAs) and the unsymmetric dimethylhydrazine (UDMHy) have to be used. As group III sources, trimethylgallium (TMGa) as well as triethylgallium (TEGa) and trimethylindium (TMIn) are applied. For solar cell device structures Te (from diethyltellurium (DETe))was used as an *n*-type dopant and Mg (from dicyclopentadienylmagnesium (Cp_2Mg)) as a *p*-dopant, respectively. For van der Pauw–Hall measurements 1–2-μm-thick test films have been grown and measured as grown and after annealing at 77 K and 300 K. Secondary ion mass spectrometry (SIMS) analysis has been performed on selected samples in order to examine the actual incorporation of the dopants in comparison to the activated amount, measured by Hall effect measurements.

To anneal defects from the quaternary, metastable material, it needs to be thermally treated at elevated temperatures after growth. These annealing procedures have been varied in this study. We have applied annealing steps consisting of a 5–120 min TBAs stabilized anneal at 700–800°C and a subsequent unstabilized annealing step at 625°C for 25 min in the MOVPE reactor.

The lattice matching has been verified performing high-resolution x-ray diffraction (HRXRD) either for the bulk films or for multiquantum well reference samples, grown under identical conditions as the bulk structures. Transmission electron microscopy (TEM) at an acceleration voltage of 300 kV with a special dark field technique [10] was used to image the distribution of the elements as well as of the strain in (GaIn)(NAs). To explain the observed strain contrast in the samples, we calculated the strain energy of the crystal for different N–III–N as well as N–In arrangements in the framework of the valence force field (VFF) model [11,12]. The input supercell contained 6346 atoms.

Photoluminescence measurements have been performed at room temperature, exciting the sample using a cw Ar ion laser, operating at 514 nm.

Deep level transient spectroscopy (DLTS) measurements were performed in a home made system. The test structures can be set to temperatures within the range of 78–450 K. The samples were always reversed biased to −1.0 V. Traps were filled when the samples were biased to a less reverse bias of −0.15 V.

Solar cells with an area of 0.25 cm^2 and 1 cm^2 were processed. Photolithography was used to define the front grid structure of the solar cells. Ti/Pd/Ag (30 nm/30 nm/100 nm) contacts were evaporated sequentially and annealed at 360°C for 2 min. The backside contact is made of Ni/AuGe/Ni (12% Ge) (10 nm/130 nm/10 nm). The contacts are reinforced by electroplated Au. The GaAs cap layer is removed on the active cell area by means of selective etching (citric acid+H_2O (1:1 wt)/H_2O_2 =3:1). An anti-reflection coating (ARC) of MgF_2/TiO_x was applied to reduce the reflection losses. However, the thickness of the ARC used for GaAs-based solar cells is not optimized to this new material system and the correpsonding wavelength range.

Results and Discussion

Our standard solar cell material shows both lattice matching to GaAs and a 1 eV band gap at a composition of 8% In and 2.8% N [13]. To adjust the N content in the quaternary alloy, there are several different possibilities, which are detailed in a separate paper [14]. Before growth of the quaternary material, ternary (GaIn)As reference structures are grown, aiming for an In content of 8%, which can be accurately determined by XRD. With the known In incorporation coefficient, which is assumed to not alter upon the addition of N, N is added to the crystal until the lattice matching condition is fulfilled. To increase the N fraction, one can decrease the TBAs partial pressure in the reactor or increase the UDMHy partial pressure, the former one of which is done, as changing the UDMHy pressure also results in changing the growth rate. An issue when *p*-type doping parts of the final solar cell structure is the increased N incorporation under otherwise unchanged conditions as the undoped or *n*-doped samples [13]. This can be compensated for by using a different TBAs partial pressure for the *p*-type region rather than for the rest of the solar cell. The known blueshift of the band gap for (GaIn)(NAs) material [15] upon annealing at high temperatures around 700°Cin the range of 16 meV at these low In concentrations has been taken into account.

Annealing Effects on the N Ordering in (GaIn)(NAs). As a metastable material is grown, phase separation effects, elemental clustering, or local atomic ordering might be an issue and nanoanalytical characterization is necessary to characterize the structures. In TEM, the (002) reflection of cubic zinc blend materials is sensitive for the chemical composition [10]. It has been shown that deviations from a homogeneous In depth profile would be detectable if they are larger than ±10% of the amount of In present in the structure, hence in the range of ±0.8% for an 8% In containing solar cell. The sensitivity of this reflection to small variations in the N depth profile is low, as a result of which imaging with the (202) reflection has also been performed in order to be able to detect possible inhomogeneities of the N depth distribution by the strain fluctuation they would introduce rather than by their chemical constrast. A (002) dark field (DF) micrograph of a complete *p* on *n* solar cell structure after growth is shown in Fig. 1(*a*). The base, emitter, and intrinsic regions of the structure are referenced in the image. With respect to the GaAs substrate, the (GaIn)(NAs) bulk film can be seen darker under the imaging conditions chosen. As there are no contrast fluctuations detectable throughout the (GaIn)(NAs) one can conclude that the In is distributed homogenously within the structure. The corresponding TEM (202) dark field micrograph is shown in Fig. 1(*b*). Large columnar strain fields are clearly observed in the TEM DF micrograph. The strain fields have a distance of 10–20 nm from each other and are elongated in growth direction to about 50 nm. The strain undulations are found in the complete quaternary structure, independent from the carrier type and concentration. As the In is dispersed homogeneously in this sample, the only source for the strong strain undulations in the material can be the nitrogen, which is capable of introducing large strains in the material due to the shortGa–N bond length.

After annealing the sample for 5 min under As stabilization at 700°C and subsequently for 25 min at 625°C in H_2 atmosphere, the strain structure of the solar cell material does not change, as can be seen from the (202) DF micrograph of the annealed sample, which is shown in Fig. 1(*c*). The distance of the strain fields can be seen a lot clearer when looking from the top through the structure instead of using cross-sectional geometry. A plan view micrograph, using (202) dark field imaging conditions, is shown in Fig. 1(*d*). Here the dark dots correspond to the tube like strain fields. From this image, we can conclude that the strain fields are randomly distributed throughout the crystal. It is also confirmed that the distance of the strain undulations is 10–20 nm, which is similar to what has been reported to be the surprisingly short minority carrier diffusion lengths of electrons in the *p* region of (GaIn)(NAs) solar cells [6]. Besides the structural characteristics, the N chain might also act as an electronic defect in the as-grown, dilute nitride material system, limiting the minority carrier diffusion length. It is, thus, definitely worthwhile to clarify the formation mechanisms as well as find growth and/or annealing conditions, under which the N chains can be removed.

For (GaIn)(NAs) material, having an In content of 30% and a N content of 1–2%, one knows that the optical and lasing properties can be significantly improved, if the sample is annealed for 5 min at 700°C under As stabilization subsequent to the growth. Cross-sectional TEM dark field micrographs of such a quantum well

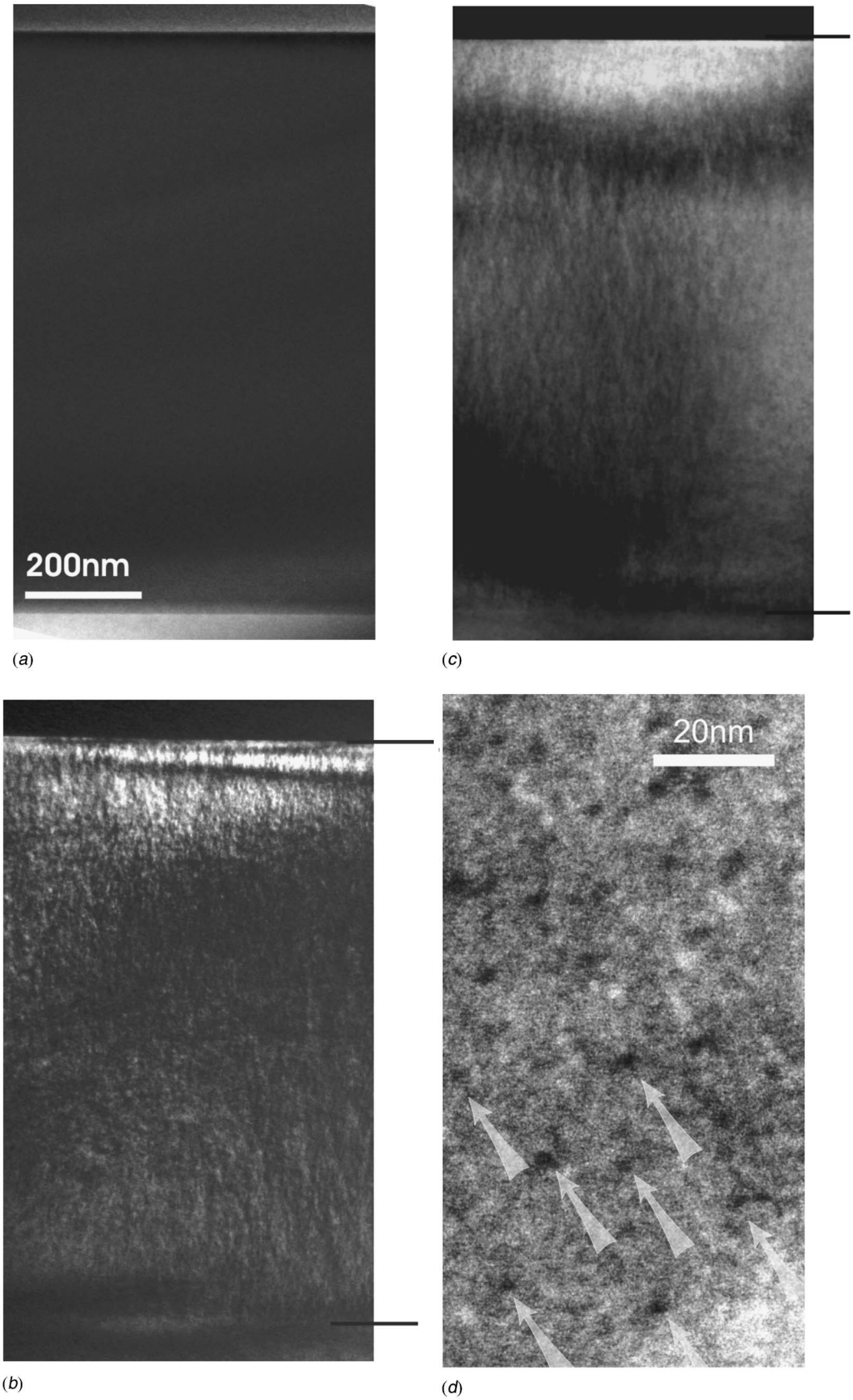

Fig. 1 Cross-sectional TEM dark field images of a $(Ga_{0.92}In_{0.08})(N_{0.03}As_{0.97})$ solar cell structure (*a*) as grown, using the (002) reflection; (*b*) as grown, using the (202) reflection; (*c*) annealed, using the (202) reflection; and (*d*) plan view TEM dark field micrograph of (GaIn)(NAs) using *g*=(202)

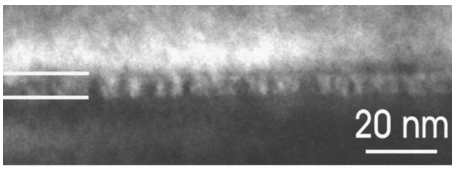

(*a*)

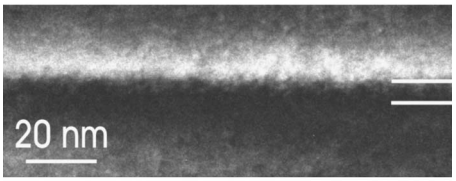

(*b*)

Fig. 2 Cross-section TEM dark field images of a $(Ga_{0.7}In_{0.3})\times(N_{0.015}As_{0.985})$ quantum well using *g*=(202) before (*a*) and after (*b*) annealing

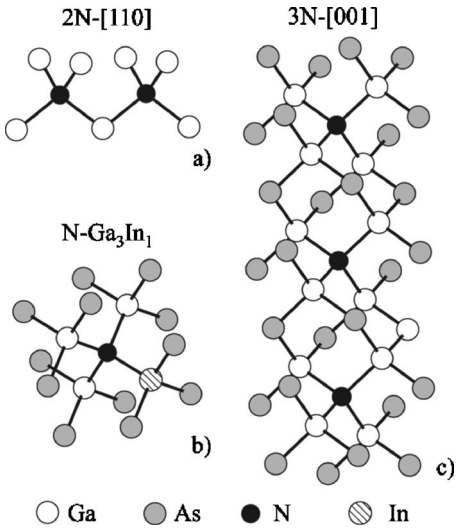

Fig. 3 Ball and stick models of different *N* configurations in Ga(NAs) and (GaIn)(NAs): (*a*) *N* nearest neighbor in [110] direction; (*b*) *N* in a 3Ga 1 In configuration; and (*c*) *N* chain, oriented in [001] direction

before (*a*) and after annealing (*b*) are depicted in Fig. 2. Due to the lower overall thickness of the quaternary material and consequently to the higher magnification used to acquire this image, the strain fields can be seen a lot clearer in this sample. There exist columnar strain fields, which again can be identified by the alternating bright/dark contrast perpendicular to the (GaIn) $\times$(NAs)/GaAs interface. In this sample the In distribution also does not show any fluctuations and hence those strain fields originate from the nitrogen. Annealing this quantum well sample has a tremendous influence on the strain distribution in the sample. After the chosen annealing procedure the columnar strain fields have disappeared completely in the high In content material studied here, which has a significantly larger In content than the solar cell structures depicted in Fig. 1.

As we identified the N to be the source of those strain fields, we performed VFF calculations of different next nearest neighbor configurations of N in GaAs and (GaIn)As. For Ga(NAs) first principle calculations have been reported in the literature [16,17]. The values for the strain of the different N configurations of our VFF calculations [18] fit very well the values reported in the literature so that we conclude that our VFF model agrees with the first principle calculations and, thus, can also be applied to calculating further configurations in In containing material. Strain fields of the extent observed cannot be explained by the lattice distortion of a single N atom in GaAs. Therefore, we concentrated on different N–N next nearest neighbor configurations and find that [011] oriented N pairs have an even higher strain energy than two separated N atoms in GaAs. Therefore this configuration should not be adopted from the crystal upon growth. In contrast to that, we find—in accordance with Refs. [16,17]–that N ordering in [001] reduces the strain energy of the crystal by 0.19 eV as compared to putting two isolated N atoms in GaAs. A ball and stick model of this [001] oriented nitrogen pair is shown in Fig. 3(*c*). The strain energy is even further reduced, when longer [001] oriented N chains in GaAs are formed. We attribute the columnar strain fields, which have the tendency to extend in growth directions and which we find in as grown Ga(NAs) as well as (GaIn) $\times$(NAs)samples of different composition, to this chain-like alignment of N upon growth into the thermodynamically stable configuration on the surface. It is important to note that these chain-like strain fields are observed for both MOVPE as well as MBE grown (GaIn)(NAs) [18] and, thus, seem to be an intrinsic property of the as-grown material.

Upon annealing, strain with respect to the GaAs substrate in the bulk layer plays a more important role and what we experimentally observe is that—under the annealing conditions used—the strain fields are dissolved for the high In containing laser material (Fig. 2(*b*)). This can also be theoretically explained by VFF calculations if we look for the influence of In on the strain in the crystal [19]. The strain of one single N atom is reduced by a factor of almost four if it goes from a 4 Ga to a 4 In next nearest neighbor configuration. By taking the bonding energy into account, which is—due to the weakness of the In–N bond—reduced for In containing material, if N is put into an In rich environment, we still calculate a significant decrease in total energy when N moves to a more In rich environment. The dissolution of the N chains, which are the stable configurations on the growth surface toward the favored In–N bonds in the bulk upon annealing are also observed experimentally. This energy difference is also the driving force for the annealing induced blueshift of the emission wavelength that is observed in the quaternary material [15]. This blueshift can be explained by a change in the N nearest neighbor configuration upon annealing, resulting in a crystal with a different band gap than the as grown one [15]. Investigations with local mode spectroscopy [20] also support this model. Upon annealing an increase of In–N bonds at the expense of Ga–N bonds is observed in these studies.

From this model, it is also possible to explain why the dissolution of the strain fields in high In containing material is easier compared to low In containing solar cell material. The probability for different In-rich environments of the N as a function of the In content is shown in Fig. 4. For structures having an In content of 30%, the probability for N having one In nearest neighbor is $>$40%, for two In nearest neighbors 27%, three In nearest neighbors 7%, and four In nearest neighbors $<$1%, respectively. Concerning material with an In content of only 8%, the probability for N to have one In nearest neighbor is 25%, for two In nearest neighbors 3%, but the probability for more In in the neighborhood is negligible in this case. Hence, upon annealing of high In content material, the N needs only to hop 0.5 nm to find an environment of two In atoms or more. In contrast to that, the N needs to cover a longer distance (1.2 nm), to reach an environment of two In atoms in the low In content material. Consequently, this diffusion process takes either longer time or only occurs at higher temperatures in low In containing material. Therefore, the annealing conditions have to be adjusted for the solar cell material to allow for a longer diffusion of the N.

Influence of Annealing Conditions on Photoluminescence Properties. We varied the annealing time between 5 min and 120 min, but the annealing temperature has been varied between

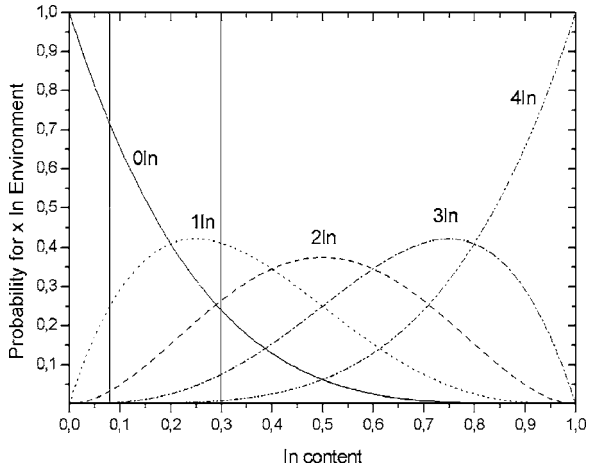

Fig. 4 Probability for different In nearest neighbor environments of nitrogen depending on the In content in the quaternary material

700°C and 850°C, always using the same TBAs partial pressure. This results in a lower As stabilization for the samples annealed at higher temperatures and hence in a more pronounced indiffusion of As vacancies, which are mediating the nearest neighbor jump of N on the group V sublattice. Increasing the anneal temperature from 700°C to 800°C while keeping the anneal time at 5 min results in an increase of Photoluminescence (PL) intensity of over two orders of magnitude (Fig. 5). Choosing even higher temperatures results in a drop of PL intensity again. This increase in PL intensity can be attributed to the anneal of defects, as e.g. N-chains, and reduction of minority carrier traps. A PL intensity gain due to altered carrier concentration can be excluded from electrical measurements. To check whether the same intensity gain can also be reached at lower temperature, but annealing for longer

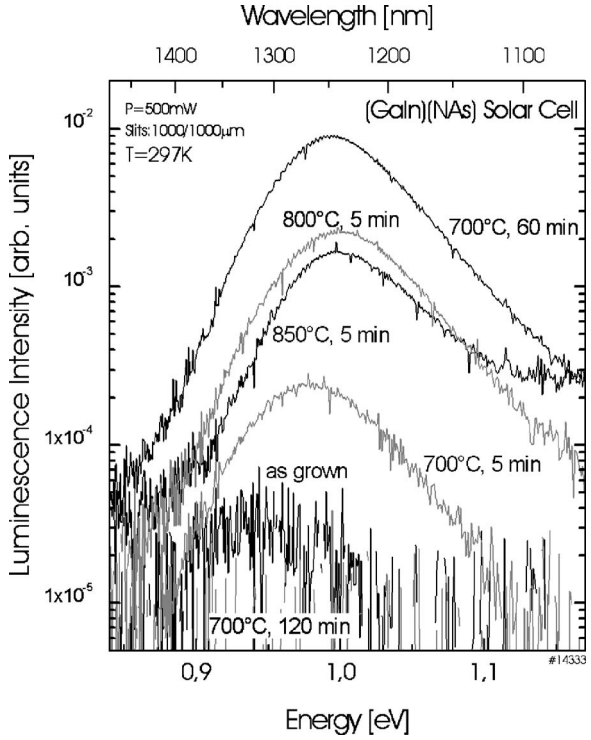

Fig. 5 Room temperature photoluminescence spectra of a $(Ga_{0.92}In_{0.08})(N_{0.03}As_{0.97})$ solar cell structure annealed under different conditions

times, the time has been varied. In conclusion, the optimum annealing conditions, which have been for high In content material 5 min at 700°C, are for low In content material 60 min at 700°C. Annealing at the same temperature for an even longer time results in a strong drop of the PL signal again, indicating that the structural and electronic properties of the sample start to deteriorate. As a result, one can conclude that the optimum annealingconditions for the (GaIn)(NAs) material system clearly depend on the In content. This is due to the fact that the N needs to hop for longer distances before it reaches a stable, In-rich local environment leading to a homogeneous distribution in the crystal and corresponding dissolution of N chain like strain fields.

Influence of the Ga Metal organic (MO) source on the Defect Characteristics by DLTS. To decide whether the Ga MO source used (TEGa or TMGa) has an influence on the defect characteristics of the solar cell material, specific DLTS structures have been grown, which consist of a 1-μm-thick (GaIn)(NAs) bulk film on a doped substrate having the same carrier type as the epitaxial layer. The nominally undoped (GaIn)(NAs) films, grown using TEGa or TMGa, respectively, show different majority carrier properties: Van der Pauw–Hall measurements yield *p*-type carrier concentrations in the range of $5-10^{*}10^{15}/cm^3$ for samples grown using TEGa. Using TMGa as source, the carrier type is *n* type with a concentration of $5-10^{*}10^{16}/cm^3$. Upon annealing for 5 min at 700°C, carrier concentration does not change for the *n*-type sample, whereas carrier concentration increases by one order of magnitude for the *p*-type, TEGa grown sample. This is presumably due to hydrogen incorporation, which passivates the acceptor upon growth, but diffuses out upon annealing.

The DLTS spectra of the TEGa grown sample before and after nonoptimzed annealing (5 min at 700°C) are shown in Fig. 6(*a*). One clearly observes a very broad defect signal at temperatures below 200 K after growth, pointing to the presence of an electron trap in these samples. The defect density is drastically reduced upon annealing, which can be seen from the disappearance of the peak for the annealed sample. The DLTS spectra of the TMGa grown samples indicate a better crystal quality using this source. After growth we find a very sharp signal slightly below 250 K corresponding to a hole trap. Upon annealing, the concentration of this defect is drastically reduced so that the DLTS spectra do not show any signal in the temperature interval measured. It has been reported very recently [21] that a N correlated defect results in a deep electron trap 0.2–0.25 eV below the band gap of the material, resulting in high dark currents and low open circuit voltages of the solar cell devices grown. It would be interesting to correlate the signal of this defect to the structural properties of the material, e.g., to the presence of N induced strain fluctuations and their removal.

Solar Cell Performance. *n*-on-*p* as well as *p*-on-*n* solar cell layer stacks have been deposited, processed, and characterized. A significant improvement of the solar cell performance upon annealing for 5 min at 700°C is observed, in accordance with the improved DLTS as well as PL-characteristics reported here.

For nonoptimal annealing conditions (700°C 5 min As stabilized, 625°C 25 min unstabilized) an open circuit voltage of 410 mV and a short circuit current of 26 mA/cm^2 under the AM1.5 global spectrum have been achieved with a *p-i-n* structure resulting in maximum efficiencies of 6%. Figure 7 shows the internal quantum efficiency (IQE) of this device. Values of up to 55% in the wavelength region of interest are promising results being in the range of the values necessary for a beneficial implementation into a four-junction solar cell. However, these results were obtained for a solar cell structure with an overall thickness of only 600 nm. This low thickness was chosen because of the poor diffusion lengths observed in the (GaIn)(NAs) material system, thereby allowing for an improved carrier collection. How-

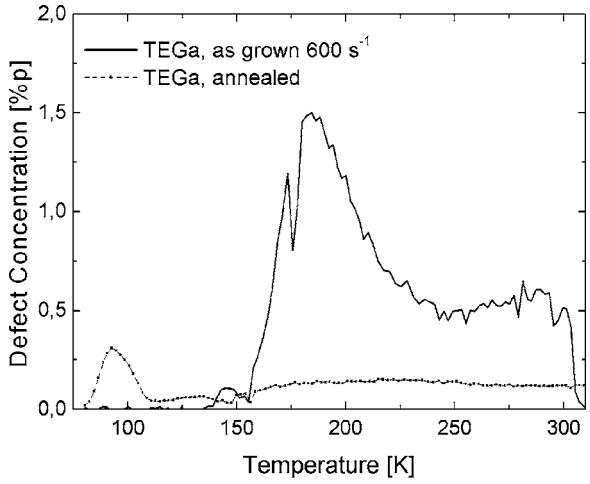

(*a*)

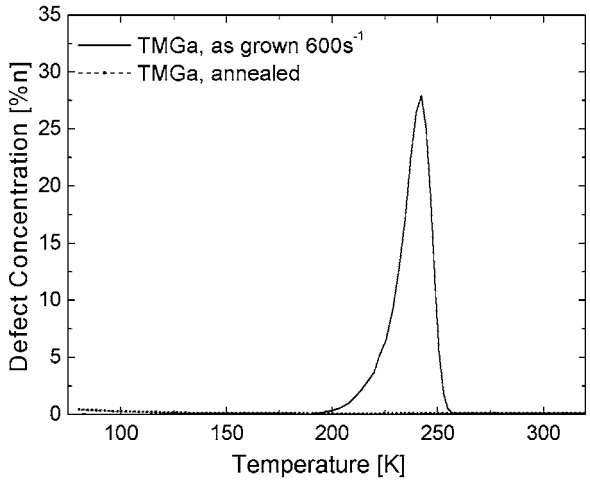

(*b*)

Fig. 6 DLTS measurements: (*a*) TEGa as grown and annealed and (*b*) TMGa as grown and annealed

ever, the low thickness in turn resulted in an incomplete absorption of the long wavelength part of the spectrum that can be seen in Fig. 7 as the IQE drops for higher wavelengths.

In a four-junction device the incident spectrum on the (GaIn) $\times$(NAs) subcell would be filtered by the layers grown above. Taking the IQE data from Fig. 7 and a filtered AM0 spectrum one

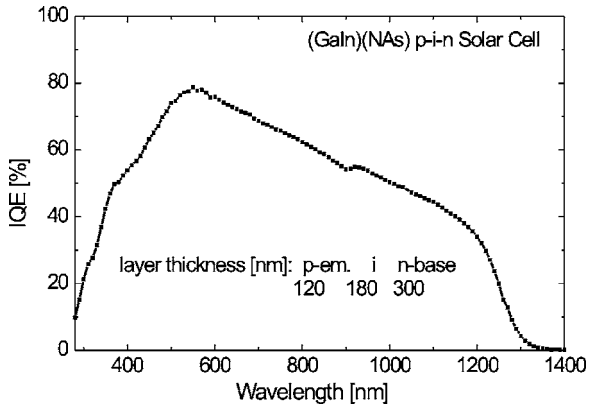

Fig. 7 IQE of a (GaIn)(NAs) pin solar cell structure

calculates about 10 mA/cm^2, whereas at least 16 mA/cm^2 would be required for an advantageous introduction into the four-junction cell. Improved electrical properties of the (GaIn)(NAs) solar cells would allow for growing solar cells of higher thicknesses while maintaining or even outperforming the high IQE values shown above. It is expected that further device improvements will result from the application of the above described optimized annealing sequence as verified in the PL investigations. These improvements will also allow for an optimized layer design improving in particular the absorption in the interested wavelength range of 900–1240 nm.

Summary

In summary, we have grown the metastable, dilute nitride alloy (GaIn)(NAs) by metalorganic vapor phase epitaxy using all liquid metalorganic precursors. The material system exhibits lattice matching to GaAs substrates, and hence to Ge, together with an energy gap of 1 eV at a composition of 8% In and 2.8% N. From the structural point of view, we find—despite a homogeneous In distribution—strong N induced strain fluctuations in the as grown material, which are an intrinsic property of dilute N containing material systems upon growth and possibly influence transport and optical properties of the material. The inhomogeneous strain fields can also be dissolved in the low In containing solar cell material using appropriate annealing conditions, which drive the N from a Ga rich environment upon growth and a stable chain-like configuration in an In rich environment, also resulting in the dissolution of the N chains. The improvements of the crystal quality upon annealing are also reflected in better photoluminescence efficiencies as well as a lower defect density in DLTS spectra in combination with improved solar cell device performance.

Acknowledgment

The authors gratefully acknowledge financial support from the European Community (IP "FULLSPECTRUM" SES6-CT-2003-502620) and the Deutsche Forschungsgemeinschaft in the framework of the topical research group on "Metastable compound semiconductor systems and heterostructures."

References

[1] Kondow, M., Uomi, K., Niwa, A., Kitatani, T., Watahiki, S., and Yazawa, Y., 1996, Jpn. J. Appl. Phys., Part 1, **35**, p. 1273.
[2] Wei, S. H., and Zunger, A., 1996, Phys. Rev. Lett., **76**, p. 664.
[3] Bellaiche, L., 1999, Appl. Phys. Lett., **75**, p. 2578.
[4] Kurtz, S. R., Myers, D., and Olson, J. M., 1997, *26th Proceedings IEEE Photovoltaic Specialists Conference*, Anaheim, Ca, IEEE, New York, p. 875.
[5] Friedman, D. J., Geisz, J. F., Kurtz, S. R., and Olson, J. M., 1998, J. Cryst. Growth, **195**, p. 409.
[6] Kurtz, S. R., Allerman, A. A., Jones, E. D., Gee, J. M., Banas, J. J., and Hammons, B. E., 1999, Appl. Phys. Lett., **74**(5), p. 729.
[7] Baur, C., Bett, A. W., Dimroth, F., Riesen, S. v., Kunert, B., Traversa, M., Volz, K., and Stolz, W., 2003, *Proc. of WCPEC-3, Osaka*, Japan, pp. 677–670.
[8] Friedman, D. J., and Kurtz, S. R., 2002, Prog. Photovoltaics, **10**, p. 331.
[9] Friedman, D. J., Geisz, J. F., Kurtz, S. R., and Olson, J. M., 1998, *Proceedings of 2nd World Conference and Exhibition on Photovoltaic Solar Energy Conversion*, Vienna, Austria.
[10] Volz, K., Torunski, T., and Stolz, W., 2005, J. Appl. Phys., **97**, p. 014306.
[11] Keating, P. N., 1966, Phys. Rev., **145**, p. 637.
[12] Martin, R. M., 1970, Phys. Rev. B, **1**, p. 4005.
[13] Volz, K., Koch, J., Kunert, B., and Stolz, W., 2003, J. Cryst. Growth, **248**, pp. 451–456.
[14] Volz, K., Koch, J., Kunert, B., and Stolz, W., 2007, J. Cryst. Growth, submitted.
[15] Klar, P. J., Grüning, H., Koch, J., Schäfer, S., Volz, K., Stolz, W., Heimbrodt, W., Kamal Saadi, A. M., Lindsay, A., and O'Reilly, E. P., 2001, Phys. Rev. B, **64**, p. 121203(R).
[16] Kent, P. R. C., and Zunger, A., 2001, Phys. Rev. B, **64**, p. 115208.
[17] Persson, C., and Zunger, A., 2003, Phys. Rev. B, **68**, p. 035212.
[18] Volz, K., Torunski, T., Stolz, W., and Harris, J. S., 2007, unpublished.
[19] Rubel, O., Volz, K., Torunski, T., Baranovskii, S. D., Grosse, F., and Stolz, W., 2004, Appl. Phys. Lett., **85**(24), p. 5908.
[20] Kurtz, S., Webb, J., Gedvilas, L., Friedman, D., Geisz, J., Olson, J., King, R., Joslin, D., and Karam, N., 2001, ' Appl. Phys. Lett., **78**, p. 748.
[21] Kurtz, S., Johnston, S., and Branz, H. M., 2005, Appl. Phys. Lett., **86**, p. 113506.